Applied Thermal Engineering 30 (2010) 1937–1945

Contents lists available at ScienceDirect

Applied Thermal Engineering

journal homepage: www.elsevier.com/locate/apthermeng

Multi-objective optimization of shell and tube heat exchangers

Sepehr Sanaye*, Hassan Hajabdollahi

Energy Systems Improvement Laboratory (ESIL), Department of Mechanical Engineering, Iran University of Science and Technology (IUST), Narmak, Tehran 16844, Iran

ARTICLE INFO

Article history:
Received 25 January 2010
Accepted 14 April 2010
Available online 21 April 2010

Keywords:
Shell and tube heat exchanger
Heat recovery
Effectiveness
Total cost
Multi-objective optimization
NSGA-II

ABSTRACT

The effectiveness and cost are two important parameters in heat exchanger design. The total cost includes the capital investment for equipment (heat exchanger surface area) and operating cost (for energy expenditures related to pumping). Tube arrangement, tube diameter, tube pitch ratio, tube length, tube number, baffle spacing ratio as well as baffle cut ratio were considered as seven design parameters. For optimal design of a shell and tube heat exchanger, it was first thermally modeled using ϵ–*NTU* method while Bell–Delaware procedure was applied to estimate its shell side heat transfer coefficient and pressure drop. Fast and elitist non-dominated sorting genetic algorithm (NSGA-II) with continuous and discrete variables were applied to obtain the maximum effectiveness (heat recovery) and the minimum total cost as two objective functions. The results of optimal designs were a set of multiple optimum solutions, called 'Pareto optimal solutions'. The sensitivity analysis of change in optimum effectiveness and total cost with change in design parameters of the shell and tube heat exchanger was also performed and the results are reported.

1. Introduction

Shell and tube heat exchanger is widely used in many industrial power generation plants as well as chemical, petrochemical, and petroleum industries. There are effective parameters in shell and tube heat exchanger design such as tube diameter, tube arrangement, baffle spacing and baffle cut ratio. Some authors considered the cost of heat transfer surface area or capital investment as an objective function to be minimized [1,2]. While others considered the sum of investment (related to the heat transfer surface area) and operational (fluid head losses) costs as an objective function for optimizing a shell and tube heat exchanger [3–8]. The sum of entropy generation of streams as an objective function was also reported in [9–11]. Multi-objective optimization of total annualized cost and the amount of cooling water required for shell and tube heat exchanger was studied in reference [12]. Hilbert et al. [13] also, used a multi-objective optimization technique to maximize the heat transfer rate and to minimize the pressure drop in a tube bank heat exchanger. Liu and Cheng [14], optimized a recuperator for the maximum heat transfer effectiveness as well as minimum exchanger weight and pressure loss.

In this paper after thermal modeling of an industrial shell and tube heat exchanger (using ϵ–*NTU* method and Bell–Delaware approach for estimating the shell side heat transfer coefficient and pressure drop), the exchanger was optimized by maximizing the effectiveness as well as minimizing the total cost. Genetic algorithm optimization technique was applied to provide a set of Pareto multiple optimum solutions. The sensitivity analysis of change in optimum values of effectiveness and total cost with change in design parameters was performed and the results are reported.

As a summary, the followings are the contribution of this paper into the subject:

- Multi-objective optimization of shell and tube heat recovery heat exchanger was performed with effectiveness and total cost as two objectives (not selected in other available literature) using genetic algorithm.
- The tube arrangement, tube diameter, tube pitch ratio, tube length, tube number, baffle spacing ratio as well as baffle cut ratio were selected as design parameters (not selected as a group of variables in other available literature).
- A closed form equation for the total cost in term of effectiveness at the optimal design point was proposed. This equation can be modified without change in its procedure of deriving for any new input values.
- Sensitivity analysis of change in objective functions when the optimum design parameters vary was performed.

2. Thermal modeling

The heat exchanger effectiveness for our selected E type TEMA shell and tube heat exchanger was estimated from [15]:

* Corresponding author. Tel./fax: +98 21 77240192.
E-mail address: sepehr@iust.ac.ir (S. Sanaye).

1359-4311/$ – see front matter © 2010 Elsevier Ltd. All rights reserved.
doi:10.1016/j.applthermaleng.2010.04.018

Nomenclature

$A_{o,t}$	tube side flow area per pass (m^2)
A_t	total tube outside heat transfer area (m^2)
A_s	cross flow area at or near the shell centerline
BC	baffle cut (m)
c_p	specific heat in constant pressure (j/kg K)
C_{min}	minimum of C_h and C_c (W/K)
C_{max}	maximum of C_h and C_c (W/K)
C^*	heat capacity rate ratio (C_h/C_{max})
C_{in}	Total investment cost ($)
C_{op}	Total operating cost ($)
C_o	annual operating cost ($/yr)
C_{total}	total cost ($)
CL	tube layout constant (−)
CTP	tube count calculation constant (−)
d_i	tube side inside diameter (m)
d_o	tube side outside diameter (m)
D_s	shell diameter (m)
f	friction factor (−)
h_i	tube side heat transfer coefficient (W/m^2 K)
h_o	shell side heat transfer coefficient (W/m^2 K)
i	annual discount rate (%)
j	Culburn number (−)
K_c	entrance pressure loss coefficient (−)
K_e	exit pressure loss coefficient (−)
k_{el}	price of electrical energy ($/kWh)
k	thermal conductivity (W/m k)
L	tube length (m)
L_{bc}	baffle spacing (m)
m	mass flow rate (kg/s)
ny	equipment life (yr)
n_p	number of tube pass (−)
N_t	number of tube (−)
NTU	number of transfer units (−)
p_t	tube pitch (m)
P	pumping power (W)
Pr	Prandtl number (−)
$R_{o,f}$	fouling resistance shell side (m^2 K/W)
$R_{i,f}$	fouling resistance tube side (m^2 K/W)
Re	Reynolds number (−)
T	temperature (°C)
U	overall heat transfer coefficient (W/m^2 K)

Greek abbreviation

ϵ	thermal effectiveness (−)
Δp	pressure drop (pa)
μ	viscosity (pa s)
η	pump efficiency (−)
τ	hours of operation per year (h/yr)
σ	ratio of minimum free flow area to frontal area (−)

Subscripts

s	shell-side
t	tube side
w	tube wall
i	inner or inlet
o	outer or outlet

$$\epsilon = \frac{2}{\left(1+C^*\right) + \left(1+C^{*2}\right)^{0.5} \coth\left(\frac{NTU}{2}\left(1+C^{*2}\right)^{0.5}\right)} \tag{1}$$

where the heat capacity ratio (C^*), and the number of transfer units (NTU), are defined as:

$$NTU_{max} = \frac{U_o A_t}{C_{min}} \tag{2}$$

$$C^* = \frac{C_{min}}{C_{max}} = \frac{\min(C_s, C_t)}{\max(C_s, C_t)} = \frac{\min((\dot{m}c_p)_s, (\dot{m}c_p)_t)}{\max((\dot{m}c_p)_s, (\dot{m}c_p)_t)} \tag{3}$$

where A_t is the total tube outside heat transfer surface area and U_o is the overall heat transfer coefficient which are computed from:

$$A_t = \pi L d_o N_t \tag{4}$$

$$U_o = \frac{1}{\frac{1}{h_o} + R_{o,f} + \frac{d_o \ln(d_o/d_i)}{2\,k_w} + R_{i,f}\frac{d_o}{d_i} + \frac{1}{h_i}\frac{d_o}{d_i}} \tag{5}$$

where L, N_t, d_i, d_o, $R_{i,f}$, $R_{o,f}$, k_w are tube length, tube number, tube inside and outside diameter, tube and shell side fouling resistances and thermal conductivity of tube wall respectively.

2.1. Tube side

The tube side heat transfer coefficient (h_i) was estimated from [15]:

$$h_i = h_t = (k_t/d_i)0.024 Re_t^{0.8} Pr_t^{0.4} \quad \text{for } 2500 < Re_t < 1.24 \times 10^5 \tag{6}$$

where k_t and Pr_t are tube side fluid thermal conductivity and Prandtl number, also Re_t is tube flow Reynolds number which is defined as:

$$Re_t = \frac{m_t d_i}{\mu_t A_{o,t}} \tag{7}$$

where m_t is the mass flow rate and $A_{o,t}$ is the tube side flow cross section area per pass estimated as:

$$A_{o,t} = 0.25\,\pi\, d_i^2 N_t / n_p \tag{8}$$

and n_p is the number of tube passes.

Furthermore, the tube side pressure drop was also estimated from [15]:

$$\Delta p_t = \frac{G^2}{2\rho_i}\left[\left(1-\sigma^2+K_c\right) + 2(\rho_i/\rho_o - 1) + \frac{4 f_t L}{d_i}\rho_i (1/\rho)_m - \left(1-\sigma^2-K_e\right)\rho_i/\rho_o\right] \tag{9}$$

where Δp_t included the pressure drop due to flow contraction, acceleration, friction, and expansion, four terms in Eq. (9). K_c and K_e are tube entrance and exit pressure loss coefficients. Furthermore f_t is the tube side friction factor estimated as:

Table 1
Geometrical properties of tube banks common in shell and tube exchangers [15].

$TLA = 30^\circ$ (Triangle)	$TLA = 45^\circ$ (Rotated Square)	$TLA = 90^\circ$ (Square)
p_t	$\sqrt{2}p_t$	p_t
$(\frac{\sqrt{3}}{2})p_t$	$\frac{p_t}{\sqrt{2}}$	p_t

$$f_t = 0.00128 + 0.1143(\mathrm{Re_t})^{-0.311} \quad (10)$$

That is accurate in range of $4000 < \mathrm{Re_t} < 10^7$ within ±2%.

2.2. Shell side

The shell diameter was estimated from [16]:

$$D_s = 0.637\, p_t \sqrt{(\pi N_t) CL/CTP} \quad (11)$$

where p_t is tube pitch and CL is tube layout constant that has a unit value for 45° and 90° tube arrangement and 0.87 for 30° and 60° tube arrangement. Also CTP is tube count constant which is 0.93, 0.9, 0.85 for single pass, two passes and three passes of tubes, respectively [17].

Bell–Delaware method was used in this paper to compute the shell side heat transfer coefficient and pressure drop in form of:

$$h_o = h_s = h_{id} J_c J_l J_b J_s J_r \quad (12)$$

where h_{id} is the heat transfer coefficient for the ideal exchanger with pure cross flow stream over tube bundle evaluated at a Reynolds number at or near the centerline of the shell in form of reference [17].

$$h_{id} = j_s c_{p,s} \left(\frac{m_s}{A_s}\right) \left(\frac{k_s}{c_{p,s}\mu_s}\right)^{2/3} \left(\frac{\mu_s}{\mu_{s,w}}\right)^{0.14} \quad (13)$$

where j_s is ideal tube bank Culburn factor, A_s is the cross flow area at or near the shell centerline (Table 1), $\mu_s/\mu_{s,w}$ is viscosity ratio at bulk to wall temperature in the shell side.

The total shell side pressure drop was computed as the sum of three terms including crossflow pressure drop (Δp_{cr}), inlet and outlet pressure drop (Δp_{i-o}) and window section pressure drop (Δp_w) as follow:

$$\Delta p_s = \Delta p_{cr} + \Delta p_{i-o} + \Delta p_w \quad (14)$$

Details of computing pressure drop, Culburn factor, friction factor and cross flow area at or near the shell centerline are referred in reference [17]. The above defined coefficient factors depend on the tube arrangement and Reynolds number. J_c is the correction factor for baffle configuration (baffle cut and spacing) and takes into account the heat transfer in the window. J_l is the correction factor for baffle leakage effects and takes into account both the shell-to-baffle and tube-to-baffle hole leakages. J_b is the correction factor for bundle and pass partition bypass streams and depends on the flow bypass area and number of sealing strips. J_s is the correction factor for bigger baffle spacing at the shell inlet and outlet sections. J_r is the correction factor for the adverse temperature gradient in laminar flows (at low Reynolds numbers) [15].

3. Genetic algorithms for multi-objective optimization

3.1. Multi-objective optimization

A multi-objective problem consists of optimizing (i.e., minimizing or maximizing) several objectives simultaneously, with a number of inequality or equality constraints. The problem can be formally written as follows:

$$\text{Find } x = (x_i) \forall i = 1, 2, \ldots, N_{\text{param}} \quad (15)$$

such as $f_i(x)$ is a minimum(respectively maximum) $\forall i = 1, 2, \ldots, N_{\text{obj}}$

Subject to:

$$g(x) \le 0 \quad \forall j = 1, 2, \ldots, M, \quad (16)$$

$$h_k(x) = 0 \quad \forall k = 1, 2, \ldots, K, \quad (17)$$

where x is a vector containing the N_{param} design parameters, $(f_i)_{i=1,\ldots,N_{\text{obj}}}$ the objective functions and N_{obj} the number of objectives. The objective function $(f_i)_{i=1,\ldots,N_{\text{obj}}}$ returns a vector containing the set of N_{obj} values associated with the elementary objectives to be optimized simultaneously. The GAs are semi-stochastic methods, based on an analogy with Darwin's laws of natural selection [18]. The first multi-objective GA, called vector evaluated GA (or VEGA), was proposed by Schaffer [19]. An algorithm based on non-dominated sorting was proposed by Srinivas and Deb [20] and called non-dominated sorting genetic algorithm (NSGA). This was later modified by Deb et al. [21] which eliminated higher computational complexity, lack of elitism and the need for specifying the sharing parameter. This algorithm is called NSGA-II which is coupled with the objective functions developed in this study for optimization.

3.2. Tournament selection

Each individual competes in exactly two tournaments with randomly selected individuals, a procedure which imitates survival of the fittest in nature.

3.3. Controlled elitism sort

To preserve diversity, the influence of elitism is controlled by choosing the number of individuals from each subpopulation, according to the geometric distribution [22],

$$S_q = S\frac{1-c}{1-c^w} c^{q-1}, \quad (18)$$

to form a parent search population, P_{t+1} ($t$denote the generation), of size S, where $0 < c < 1$. w is the total number of ranked non-dominated and q is the total number of new parent sections.

3.4. Crowding distance

The crowding distance metric proposed by Deb [23] is utilized, where the crowding distance of an individual is the perimeter of the rectangle with its nearest neighbors at diagonally opposite corners. So, if individual $X^{(a)}$ and individual $X^{(b)}$ have same rank, each one has a larger crowding distance is better.

3.5. Crossover and mutation

Uniform crossover and random uniform mutation are employed to obtain the offspring population, Q_{t+1}.The integer-based uniform crossover operator takes two distinct parent individuals and interchanges each corresponding binary bits with a probability, $0 < p_c \le 1$. Following crossover, the mutation operator changes each of the binary bits with a mutation probability, $0 < p_m < 0.5$.

Table 2
The operating conditions of the shell and tube heat exchanger (input data for the model).

Thermophysical and process data	Shell side (hot stream) (oil)	Tube side (cold stream) (water)
Density (kg/m^3)	860	995
Specific heat (j/kg K)	2115	4120
Viscosity	0.0643	0.000695
Thermal conductivity (W/m K)	0.14	0.634
Fouling factor m^2 W/K	0.00015	0.000074

4. Objective functions, design parameters and constraints

In this study the effectiveness and total cost were considered as two objective functions. Total cost included the investment cost of heat transfer surface area as well as the operating cost for the pumping power.

$$C_{total} = C_{in} + C_{op} \tag{19}$$

The total investment cost for both shell and tube (stainless steel) was [24]:

$$C_{in} = 8500 + 409A_t^{0.85} \tag{20}$$

where A_t is the total tube outside heat transfer surface area.

The total operating cost related to pumping power to overcome friction losses of both hot and cold streams was computed from [7]:

$$C_{op} = \sum_{k=1}^{ny} \frac{C_o}{(1+i)^k} \tag{21}$$

$$C_o = P\, k_{el}\, \tau \tag{22}$$

$$P = \frac{1}{\eta}\left(\frac{m_t}{\rho_t}\Delta p_t + \frac{m_s}{\rho_s}\Delta p_s\right) \tag{23}$$

where ny is the equipment life time in year, i is annual discount rate, k_{el}, τ and η are price of electrical energy, hours of operation per year and the pump efficiency, respectively. In this study tube arrangement, tube diameter, tube pitch ratio p_t/d_o, tube length, tube number, baffle spacing ratio ($L_{bc}/D_{s,i}$) as well as baffle cut ratio ($BC/D_{s,i}$) were considered as seven design parameters. The following constraint was introduced to insure that the ratio of tube length (in one pass) to the shell diameter, changes in the following range of:

$$(L/D_s)_{min} < L/D_s < (L/D_s)_{max} \tag{24}$$

Typical values are considered 3 and 12 for lower and upper limits, respectively.

5. Case study

The optimum design parameters were obtained for an oil cooler shell and tube heat recovery heat exchanger in Sarcheshmeh cupper production power plant located in south of Kerman city. The goals in this study were to maximize effectiveness while minimizing the total cost. The oil (hot stream, c_p = 2115 j/kg K) mass flow rate was 8.1 kg/s with 78.3 °C inlet temperature entered the shell side. The fresh water (cold stream, c_p = 4120 j/kg K) with 12.5 kg/s mass flow rate at 30 °C entered the tube side. The operating conditions are listed in Table 2. In this study the equipment life period was ny = 10 yr, the rate of annual discount was i = 10%, the price of electricity was k_{el} = 0.15 $/kWh and hours of operation and pump efficiency were τ = 7500 h/yr and η = 0.6 respectively. Three tube arrangements (30°, 45°, 90°) and 20 various standard tube diameters (with definite inner and outer diameter listed in Table 3) were considered as discrete design variables [25].

Table 3
Inner and outer diameters (d_i, d_o) in inches for 20 standard tubes.

(0.444, 1/2)	(0.407, 5/8)	(0.435, 5/8)	(0.481, 5/8)
(0.495, 5/8)	(0.509, 5/8)	(0.527, 5/8)	(0.541, 5/8)
(0.555, 5/8)	(0.482, 3/4)	(0.510, 3/4)	0.532, 3/4)
(0.560, 3/4)	(0.584, 3/4)	(0.606, 3/4)	(0.620, 3/4)
(0.634, 3/4)	(0.352, 3/4)	(0.680, 3/4)	(0.607, 7/8)

Table 4
Comparison of modeling output and the corresponding results from reference [15].

Variables	Unit	Reference [15]	Present paper	Difference(%)
ϵ	–	0.1555	0.1599	2.83
C_{total}	$	74,598	74,112	0.65
Δp_t	kPa	17.58	17.660	0.45
Δp_s	kPa	112	111.02	−0.875
q	kW	393.6	404.63	2.78
h_t	W/m^2 K	7837	7838.2	0.0153
h_s	W/m^2 K	698.8	730.226	4.497

6. Discussion and results

6.1. Verification of modeling and optimization results

To verify the modeling results, the simulation output was compared with the corresponding reported results given in literature. The comparison of our modeling results and the corresponding values from reference [15], for the same input values is shown in Table 4. Results show that the difference percent points of modeling output results obtained in this paper and that given in reference [15] are acceptable for both objective functions (effectiveness and total cost).

6.2. Optimization results

To maximize the effectiveness value and to minimize the total cost, seven design parameters including, tube arrangement, tube diameter, tube pitch ratio, tube length, tube number, baffle spacing ratio as well as baffle cut ratio were selected. Design parameters (decision variables) and the range of their variations are listed in Table 5. The number of iterations for finding the global extremum in the whole searching domain was about 8.2 × 10^{15}. The genetic algorithm optimization was performed for 200 generations, using a search population size of M = 100 individuals, crossover probability of p_c = 0.9, gene mutation probability of p_m = 0.035 and controlled elitism value c = 0.65. The results for Pareto-optimal curve are shown in Fig. 1, which clearly reveal the conflict between two objectives, the effectiveness and the total cost. This concept is also pointed out in reference [26]. Any geometrical change that

Table 5
The design parameters, their range of variation and their change step.

Variables	From	To	Step of change
Tube arrangement	(30°, 45°, 90°)	(–)	1
Tube inside diameter m	0.0112	0.0153	–
p_t/d_o	1.25	2	0.001
Tube length m	3	8	0.001
Tube number	100	600	1
Baffle cut ratio	0.19	0.32	0.001
Baffle spacing ratio	0.2	1.4	0.001

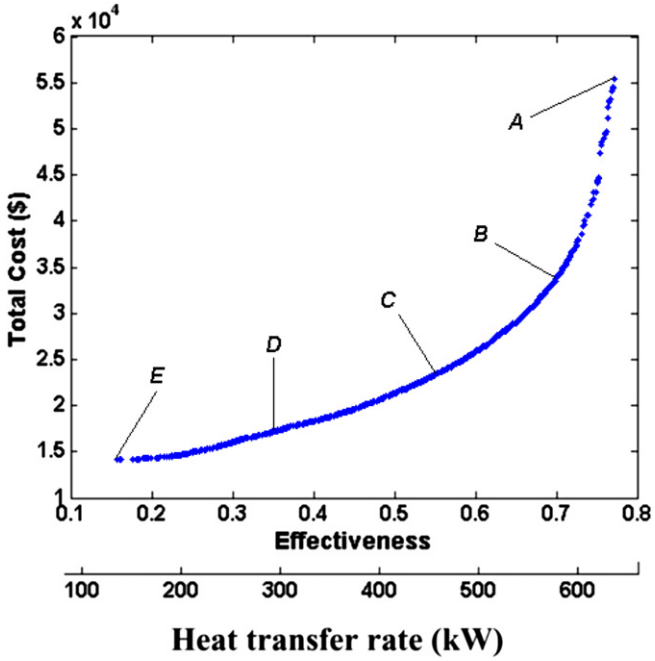

Fig. 1. The distribution of Pareto-optimal points solutions using NSGA-II.

increases the effectiveness or heat recovery of the heat exchanger ($\epsilon = q/q_{max}$, $q = 827.45\ \epsilon$(kW) in this case), leads to an increase in the total cost and vice versa. This shows the need for multi-objective optimization techniques in optimal design of a shell and tube heat exchanger. It is note worthy that Fig. 1 shows the minimum values of total cost ($) with (effectiveness or) heat transfer rate (kW) for various points on Pareto optimal front. Results show that the heat transfer rate changes in the range of 130.3 (kW) to 638.1 (kW) in our case study. Therefore for specific heat transfer rate, the reported results are applicable for a problem with one objective function (the total cost) and specific constraint (the value of selected or input heat transfer rate). This means that the presented multi-objective optimization method provides a general optimal solution which in simplified form, one may obtain an optimum design (minimum of the total cost) for a specified heat transfer rate.

It is shown in Fig. 1, that the maximum effectiveness (maximum heat recovery) exists at design point *A* (0.7712), while the total cost is the biggest at this point. On the other hand the minimum total cost occurs at design point *E* (14,109 $), with a smallest effectiveness value (0.1575) (minimum heat recovery) at that point. Design point *A* is the optimal situation at which, effectiveness is a single objective function, while design point *E* is the optimum condition at which total cost is a single objective function.

Optimum total cost and effectiveness (heat recovery) for five typical points from *A* to *E* Pareto-optimal fronts for input values given in Table 2 are listed in Table 6.

To provide a useful tool for the optimal design of the shell and tube heat exchanger, the following equation for effectiveness versus the total cost was derived for the Pareto curve (Fig. 1).

$$C_{total}(\$) = \frac{-0.2478\,\epsilon^2 - 1.238\,\epsilon + 1.19}{\epsilon^2 - 2.093\,\epsilon + 1.035} \times 10000 \quad (25)$$

Equation (25) is valid in the range of $0.1575 < \epsilon < 0.7712$ for effectiveness. The interesting point in equation (25) is that considering a numerical value for the effectiveness in mentioned range, provides the minimum total cost for that optimal point along with other optimal design parameters. It is note worthy that this equation can be modified without change in its procedure of deriving for new given input values.

The selection of final solution among the optimum points existing on the Pareto front needs a process of decision-making. In fact, this process is mostly carried out based on engineering experiences and importance of each objective for decision makers. In this paper based on information provided for designers (The practical effectiveness values in the range of $0.55 < \varepsilon < 0.7$), the design points (*B*–*C*) with reasonable total cost and effectiveness values are recommended.

Distribution of variables for Pareto front (Fig. 1) is shown in Fig. 2a–g.

Lower and upper bounds of the variables are shown by dotted lines.

The selected tube arrangement was 30° which improved both objective functions simultaneously. Since the optimum values of decision variables (except tube arrangement) have scattered distribution in their whole allowable domains, one may predict that these six parameters have important effects on the conflict between the higher values of effectiveness and lower amounts of the total cost.

The variation of optimum values of effectiveness with the total cost for various values of optimum design parameters in *A*–*E* cases (Pareto front) is shown in Fig. 3a–e. It was observed that the variation of two objective functions at other points on Pareto optimal front had the same trend as the five points (*A*–*E*). The effect of design variables on objective functions is investigated and explained as follows:

6.2.1. Tube pitch ratio

By increasing p_t/d_o, both effectiveness and total cost decreased for all design points *A*–*E* (Fig. 3a) with moderate slope. Therefore, variations of tube pitch ratio cause a conflict between two objective functions and values of tube pitch ratio have scattered distribution (especially around its minimum value) in the allowable domain (Fig. 2c).

6.2.2. Tube length

By increasing the tube length, both effectiveness and total cost increase for all design points *A*–*E* (Fig. 3b). Therefore, variations of tube length cause a conflict between two objective functions and values of tube length have scattered distribution in the whole allowable domain (Fig. 2d).

6.2.3. Tube number

Similar to the tube length, both effectiveness and the total cost increase with increasing the tube number (Fig. 3c). Therefore the tube number caused a conflict between two objective functions and

Table 6
The optimum values of effectiveness and the total cost for the design points A to E in Pareto-optimal fronts for input values given in Table 2.

	A	B	C	D	E
Effectiveness	0.77119	0.69965	0.55044	0.34938	0.15748
Heat recovery (kW)	638.1212	578.9254	455.4616	289.0945	130.3068
Total Cost ($)	55,359	33,729	23,328	17,169	14,109

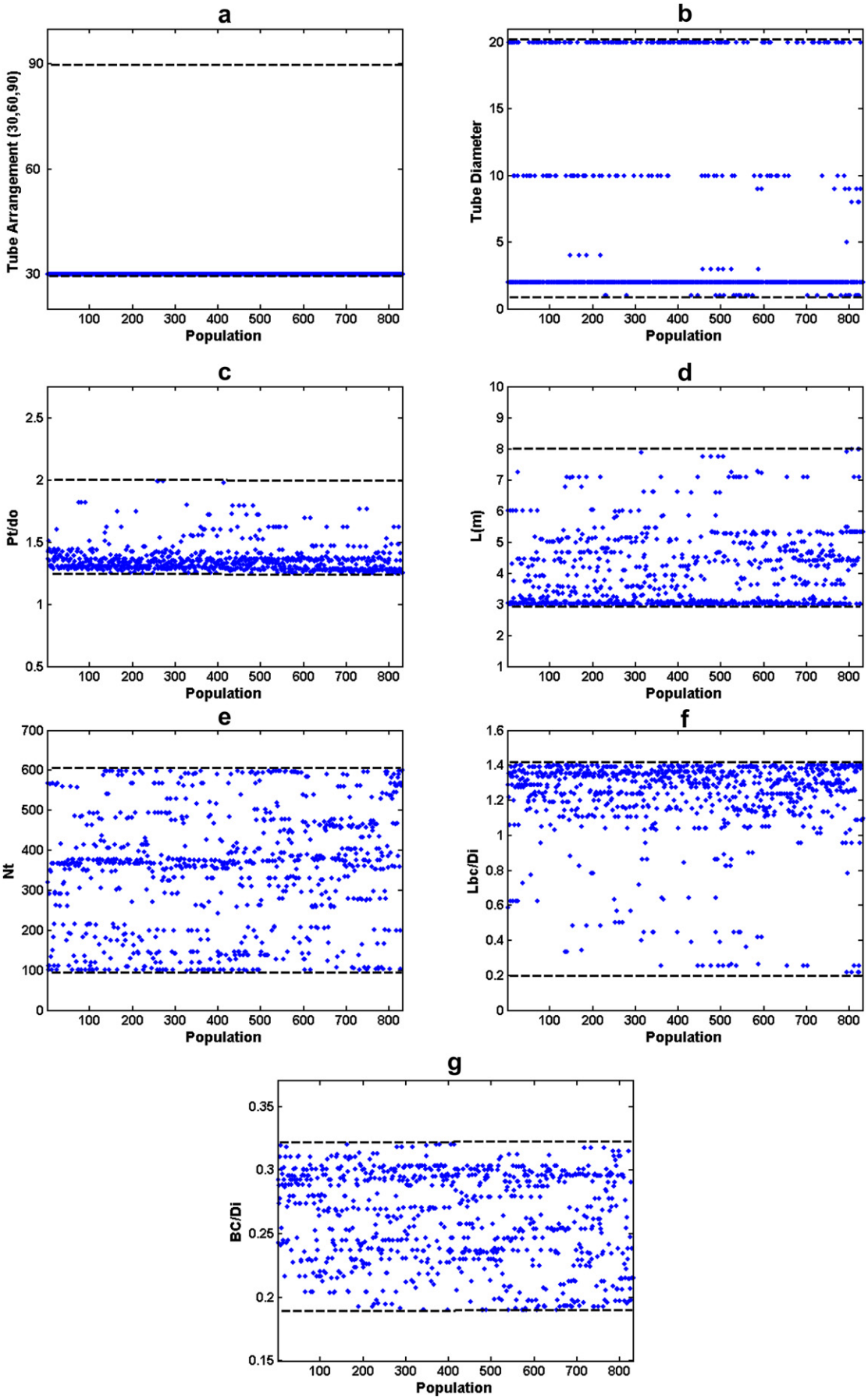

Fig. 2. Scattering of variables for the Pareto optimal front a. tube arrangement, b. tube diameter, c. tube pitch ratio, d. tube length, e. tube number, f. baffle spacing ratio, g. baffle cut ratio.

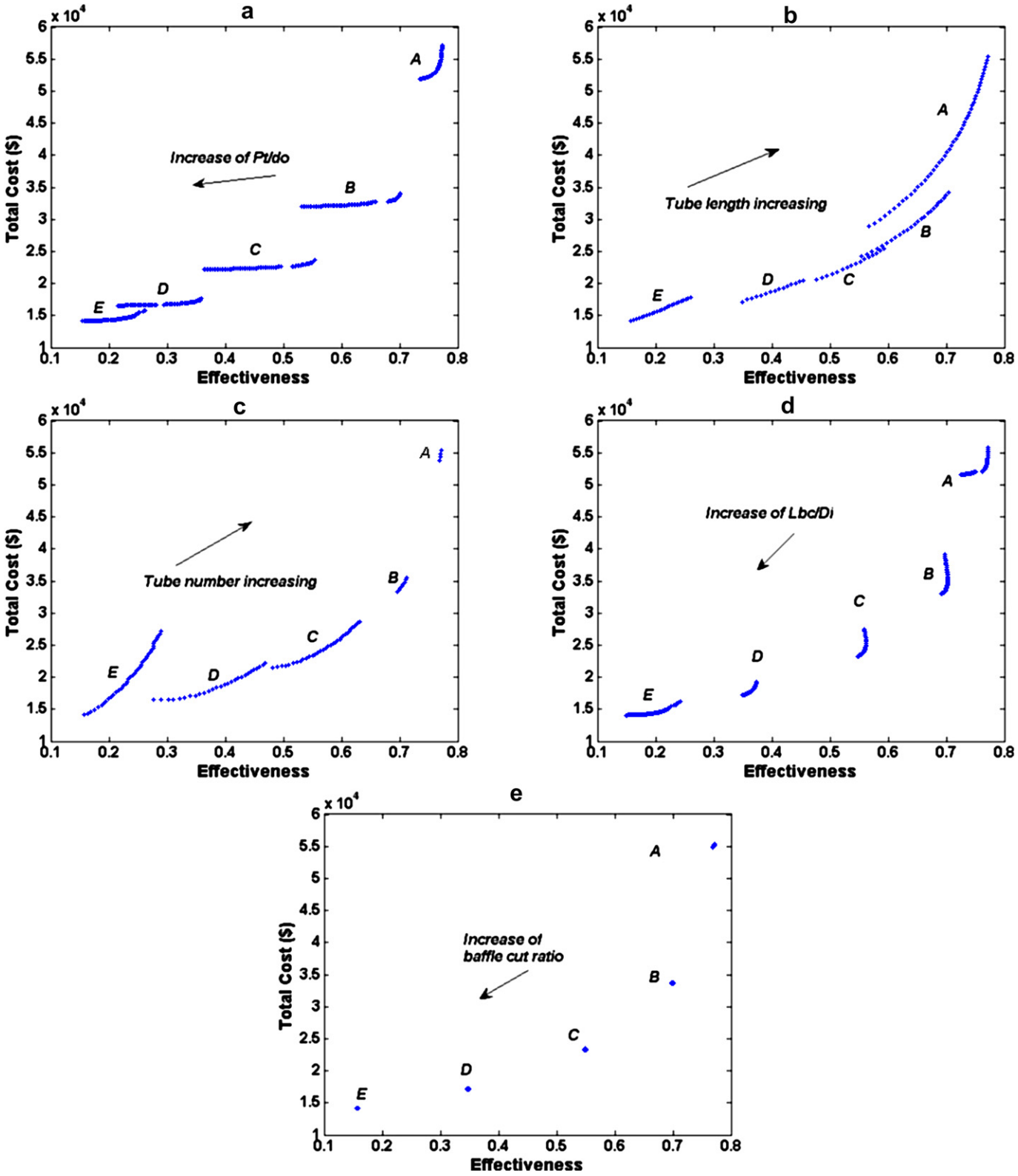

Fig. 3. The variation of effectiveness with the total cost for five optimum design parameters in five cases of A–E. a. tube pitch ratio, b. tube length, c. tube number, d. baffle spacing ratio, e. baffle cut ratio.

the tube number values obtained on Pareto optimal front have scattered distribution as shown in Fig. 2e.

6.2.4. Baffle spacing ratio

As shown in Fig. 3d, an increase in the baffle spacing ratio ($L_{bc}/D_{s,i}$) creates a conflict between two objective functions. Scattered distribution of baffle spacing ratio in Fig. 2f approves this point too.

6.2.5. Baffle cut ratio

Increase in baffle cut ratio (BC/$D_{s,i}$) decreases both effectiveness and total cost (Fig. 3e). This is while that this parameter had scattered distribution in the whole allowable domain, Fig. 2g.

7. Outlet temperature

The flow outlet temperature of shell and tube sides was obtained from:

$$T_{s,o} = T_{s,i} - \epsilon\frac{C_{min}}{C_s}(T_{s,i} - T_{t,i}) \quad (26)$$

$$T_{t,o} = T_{t,i} + \epsilon\frac{C_{min}}{C_t}(T_{s,i} - T_{t,i}) \quad (27)$$

where $T_{s,i}$ and $T_{s,o}$ are inlet and outlet temperatures on the shell side and $T_{t,i}$, $T_{t,o}$ are inlet and outlet temperatures on the tube side of heat exchanger, respectively. The variation of outlet temperature versus effectiveness (or heat transfer rate) for various optimal points on Pareto front is shown in Fig. 4. Therefore with a specified flow outlet temperature on shell (or tube) side, one may obtain the outlet temperature of tube (or shell) side at the optimum design point (maximum effectiveness or heat transfer rate).

It should be noted that based on Eqs. (26) and (27), the maximum value of effectiveness provides the maximum value of tube side flow outlet temperature and minimum value of shell side flow outlet temperature. Furthermore with a known effectiveness or heat transfer rate, one may obtain both cold and hot stream flow outlet temperatures for an optimal design of shell and tube heat exchanger.

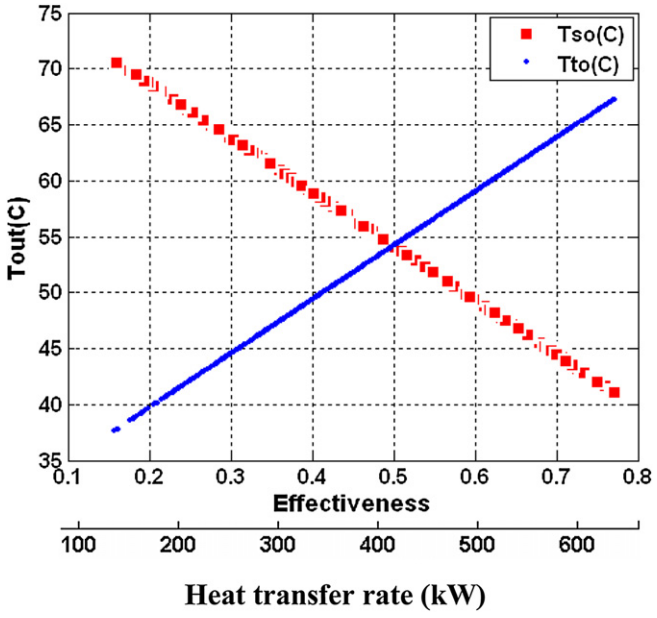

Fig. 4. Distribution of outlet temperature versus effectiveness (and heat recovery) on each side for the Pareto optimal front.

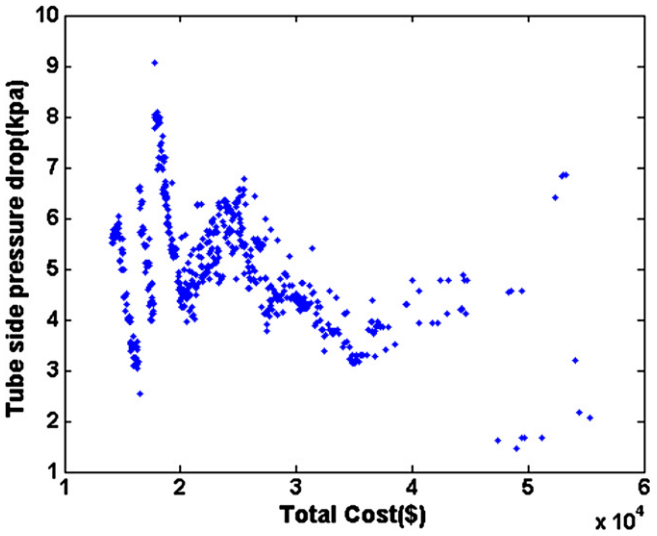

Fig. 5. Tube side pressure drop (kPa) versus the total cost ($).

8. The allowed pressure drop

In many problems there are allowed (limited) given pressure drop values in tube and/or shell sides. These values may be taken care of in optimum design procedure with the presented method. As indicated, the pressure drop was computed in both tube (Eq. (9)) and shell (Eq. (14)) sides. Then the pumping power (Eq. (23)) was obtained for estimating the operational cost (C_{op} in Eq. (19)) which is a part of one objective function (the total cost). Figs. 5 and 6 show the values of tube and shell side pressure drops versus the minimum total cost (one objective function) for various optimal points of Pareto front. Results of analyzing our case study showed that the tube side pressure drop changed in the range of 2–7 kPa and the shell side pressure drop changed in the range of 1–37 kPa. Therefore with specifying (restricting) values for tube and shell side pressure drop, the allowed Pareto front solution may be selected from Figs. 5 or 6, as possible optimal solution candidates.

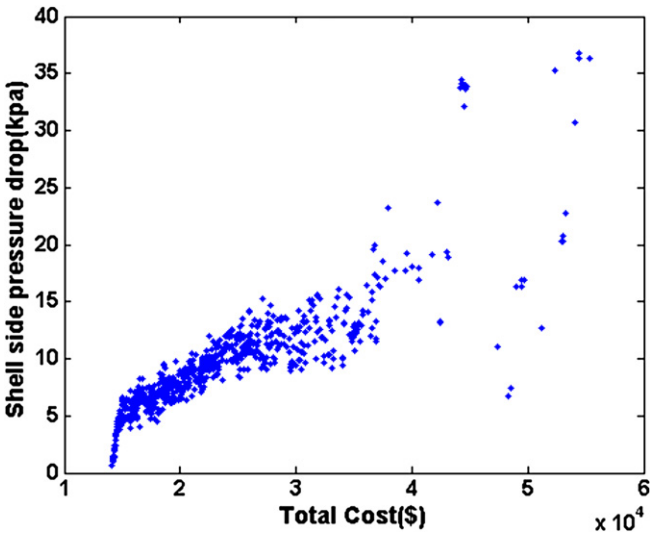

Fig. 6. Shell side pressure drop (kPa) versus the total cost ($/year).

9. Conclusions

A shell and tube heat exchanger was optimally designed by defining two objective function (total cost and effectiveness) and applying genetic algorithm technique. The effectiveness was maximized and total cost was minimized. The design parameters (decision variables) were tube arrangement, baffle cut ratio, tube pitch ratio, tube length, tube number, baffle spacing ratio as well as 20 standard tube diameters. A set of Pareto optimal points was obtained and shown. The results clearly revealed the level of conflict between two objective functions. Tube pitch ratio, tube length, tube number as well as baffle spacing ratio were found to be important design parameters which caused a conflict between the effectiveness and total cost. On the other hand, no or weak effect on the conflict between two optimized objective functions was observed for design parameters such as tube arrangement.

References

[1] L.H. Costa, M. Queiroz, Design optimization of shell-and-tube heat exchangers. Applied Thermal Engineering 28 (2008) 1798–1805.
[2] K. Ramananda Rao, U. Shrinivasa, J. Srinivasan, Synthesis of cost optimal shell-and-tube heat exchangers. Heat Transfer Engineering 12 (3) (1991) 47–55.
[3] M. Fesanghary, E. Damangir, I. Soleimani, Design optimization of shell and tube heat exchangers using global sensitivity analysis and harmony search algorithm. Applied Thermal Engineering 29 (2009) 1026–1031.
[4] J.M. Ponce-Ortega, M. Serna-Gonzalez, L.I. Salcedo-Estrada, A. Jimenez-Gutierrez, Minimum-investment design of multiple shell and tube heat exchangers using a MINLP formulation. Chemical Engineering Research and Design Part A (October 2006).
[5] J.M. Ponce-Ortega, M. Serna-Gonzalez, A. Jimenez-Gutierrez, Use of genetic algorithms for the optimal design of shell-and-tube heat exchangers. Applied Thermal Engineering 29 (2009) 203–209.
[6] M.A.S.S. Ravagnani, J.A. Caballero, Optimal heat exchanger network synthesis with the detailed heat transfer equipment design. Computers and Chemical Engineering 31 (2007) 1432–1448.
[7] A.C. Caputo, P.M. Pelagagge, P. Salini, Heat exchanger design based on economic optimization. Applied Thermal Engineering 28 (2008) 1151–1159.
[8] Y. Özçelik, Exergetic optimization of shell and tube heat exchangers using a genetic based algorithm. Applied Thermal Engineering 27 (2007) 1849–1856.
[9] A. Bejan, G. Tsatsaronis, M. Moran, Thermal design and optimization. Wiley Interscience (1995).
[10] E. Johannessen, L. Nummedal, S. Kjelstrup, Minimizing the entropy production in heat exchange. International Journal of Heat and Mass Transfer 45 (2002) 2649–2654.
[11] S. Sun, Y. Lu, C. Yan, Optimization in calculation of shell-and-tube heat exchanger. International Communication in Heat and Mass Transfer 20 (1993) 675–685.
[12] A. Agarwal, S.K. Gupta, Jumping gene adaptations of NSGA-II and their use in the multi-objective optimal design of shell and tube heat exchangers. Chemical Engineering Research and Design 86 (2008) 123–139.
[13] R. Hilbert, G. Janiga, R. Baron, D. Thevenin, Multi-objective shape optimization of a heat exchanger using parallel genetic algorithms. International Journal of Heat and Mass Transfer 49 (2006) 2567–2577.
[14] Z. Liu, H. Cheng, Multi-objective optimization design analysis of primary surface recuperator for microturbines. Applied Thermal Engineering 28 (2008) 601–610.
[15] R.K. Shah, P. Sekulic, Fundamental of Heat Exchanger Design. John Wiley & Sons, Inc, 2003.
[16] J. Taborek, Industrial heat exchanger design practices, in: Boiler Evaporators, and Condenser. Wiley, New York, 1991.
[17] S. Kakac,, H. Liu, Heat Exchangers Selection Rating, and Thermal Design. CRC Press, New York, 2000.
[18] D.E. Goldberg, Genetic Algorithms in Search, Optimization and Machine Learning. Addison-Wesley, Reading, MA, 1989.
[19] J.D. Schaffer, Multiple objective optimization with vector evaluated genetic algorithms, in: Proceedings of the International Conference On Genetic Algorithm And Their Applications, 1985.
[20] N. Srinivas, K. Deb, Multiobjective optimization using nondominated sorting in genetic algorithms. Journal of Evolutionary Computation 2 (3) (1994) 221–248.
[21] K. Deb, A. Pratap, S. Agarwal, T. Meyarivan, A fast and elitist multiobjective genetic algorithm: NSGA-II. IEEE Transactions on Evolutionary Computation 6 (2) (2002) 182–197.
[22] K. Deb, T. Goel, Controlled elitist non-dominated sorting genetic algorithms for better convergence, in: Proceedings of the First International Conference On Evolutionary Multi-Criterion Optimization, Zurich, 2001, pp. 385–399.
[23] K. Deb, Multi-objective Optimization Using Evolutionary Algorithms. John Wiley and Sons Ltd, Chichester, 2001.
[24] M. Taal, I. Bulatov, Jiri Klemes, Petr Stehlik, Cost estimation and energy price forecasts for economic evaluation of retrofit projects. Applied Thermal Engineering 23 (2003) 1819–1835.
[25] Standards of the Tubular Exchanger Manufactures Association, seventh ed.. TEMA, Tarrytown, NY, 1998.
[26] Jiangfeng Guo, Mingtian Xu, Lin Cheng, The application of field synergy number in shell-and-tube heat exchanger optimization design. Applied Energy 86 (2009) 2079–2087.